ELSEVIER

Catalysis Today 28 (1996) 3–15

CATALYSIS TODAY

Niobium oxide based materials as catalysts for acidic and partial oxidation type reactions

J.C. Védrine *, G. Coudurier [a], A. Ouqour [a], P.G. Pries de Oliveira [a,b], J.C. Volta [a]

[a] *Institut de Recherches sur la Catalyse, CNRS, 2 Avenue A. Einstein, F-69626 Villeurbanne Cédex, France*
[b] *Instituto Nacional de Tecnologia, Avenida Venezuela 82, 20081 Rio de Janeiro, Brasil*

Abstract

Niobic acid, $H_8Nb_6O_{19} \cdot xH_2O$, was synthesized and studied for its acidic features as a function of its dehydroxylation extent. It was observed to be strongly acidic, using NH_3 adsorption calorimetry and isopropanol conversion reaction as probe techniques, and to be weakly acidic on its dehydrated form, Nb_2O_5. The mixed oxide Al_2O_3:Nb_2O_5 in 1:1 molar ratio prepared from aluminum and niobium oxalates was shown to be amorphous up to 1023 K where it crystallized in the form of $AlNbO_4$ and to exhibit higher acidity than Nb_2O_5 dehydrated, as expected from Tanabe's model but much less acidic than the niobic acid form. The single Nb_2O_5 and mixed Al_2O_3:Nb_2O_5 oxides were used as supports for grafting MoO_x and VO_x species, respectively. It was observed that for MoO_x/Nb_2O_5 samples new strong acid sites were created while the redox properties were not as satisfactory as expected. For VO_x/Al_2O_3:Nb_2O_5 samples, at relatively low coverage (ca. 15%), acidic features were not appreciably modified (only slightly enhanced) while new redox features were generated resulting in a rather satisfactory mild oxidation catalyst. The degree of condensation of VO_x species on the mixed oxide surface, including some possible epitaxial grafting, even if not clearly characterized, appeared to play a determining role in oxidative dehydrogenation properties. This constitutes a new example of structure sensitivity in partial oxidation reactions on oxides.

Keywords: Niobium oxide catalysts; Oxidation

1. Introduction

Niobium is an element of which interest in catalysis remains limited at present although several congresses, books and one issue of Catalysis Today [1] have been devoted to it and have tried to assemble all experimental data on niobium compounds and on their catalytic properties. It, however, presents great potentialities for many different catalytic reactions and even an industrial process has been developed by Sumitomo Chemical Co. using Pd supported on niobic acid for methylisobutylketone formation starting from acetone [2].

The simplest compound is niobium hydroxide which transforms into niobic oxide upon dehydroxylation. Such an oxide may be mixed with other oxides to obtain materials exhibiting usually higher acidity features and forming in some cases new crystalline materials, including layer materials. Compounds as hydrides sulfides or carbides could also be synthesized exhibiting then peculiar catalytic properties.

Another aspect of such an oxide and mixed oxides is their use as a support for other com-

* Corresponding author. Tel. (+33) 72 445313, fax (+33) 72 445413.

SSDI 0920-5861(95)00213-8

pounds to get new catalysts due to the different forms of dispersed species with an eventual effect of the support either structurally (favoring an epitaxial growth of the overlayer on the surface) or electronically by modifying the supported species. Such species could be metals, oxides, etc.

In the present work, both approaches have been followed. Firstly, niobic acid and a mixed Al_2O_3:Nb_2O_5 oxide have been synthesized and studied. Secondly, such compounds have been used to support either MoO_x species or VO_x species, respectively, and their catalytic properties have been studied in partial oxidation reactions.

Niobic acid is known as an isopolyacid $H_8Nb_6O_{19} \cdot xH_2O$ which was shown previously by Tanabe and coworkers [3,4] to exhibit strong acidity because of the presence of labile protons. Upon calcination above 773 K, γ-Nb_2O_5 is known to be formed by dehydroxylation and to exhibit relatively weak acidity.

When different oxides are mixed together, materials with different acidic properties may be formed. Three different proposals have formulated to predict the acidity of mixed oxides.

(i) When the mixed oxide is an actual solid solution, the host oxide imposes its own environment of cations to the guest oxide. In this case, acidity is created if the charge of the guest cation is lower than that of the host cation, a Brønsted acidity could be created as charge balance cation. Silica–aluminas and more particularly zeolites constitute a very known example of Brønsted acidity created by the substitution of tetrahedral Si^{4+} by Al^{3+}.

(ii) According to Tanabe et al. [5,6], Lewis or Brønsted acidity may also be formed if in the host oxide, the guest cation preserves its coordination number in a surrounding of oxide ions with the coordination number of the host oxide. In such a case, acidity may appear whatever be the respective charge of the host and guest cations. Significant examples are those of TiO_2–SiO_2 [7–9], ZrO_2–SiO_2 [10,11] and Nb_2O_5–SiO_2 or Nb_2O_5–TiO_2 [12] which exhibit higher acidity than their components taken individually.

(iii) Finally, Seiyama [13] proposes that acidity appears at the boundary where two oxides contact. Each cation preserves its environment, only the oxide ion shared by the two cations exhibit a coordination number of two. This model may be applied in the case of the dispersion of an oxide on a support.

According to these three assumptions, mixing Nb_2O_5 to Al_2O_3 could generate acidity of Brønsted or Lewis type, except if the well defined $AlNbO_4$ phase [14], which presents a structure similar to that of TiO_2(B) [15], was formed.

Following Tanabe's approach, introducing Nb^{5+} into alumina where Al^{3+} cations are hexacoordinated should induce a Lewis acidity with a 3^+ positive charge on Nb^{5+} cation if Nb^{5+} is tetracoordinated as suggested in Ref. [16] or a 2^+ positive charge if Nb^{5+} is hexacoordinated.

At last, using Nb_2O_5 or Al_2O_3:Nb_2O_5 as a support, it is possible to obtain different catalysts by grafting oxidic species as MoO_x or VO_x known to present peculiar and specific properties for oxidation reactions.

2. Experimental

Niobic acid, $H_8Nb_6O_{19} \cdot xH_2O$, was prepared in the laboratory, as described in detail in Ref. [17] and [18], by hydrolysis of $NbCl_5$ (Aldrich 99% pure) in aqueous solution by NH_4OH at a pH of 7. After filtration and washing with ion-exchanged water, the sample was dried at 383 K.

Al_2O_3:Nb_2O_5 mixed oxide [19] was prepared starting from $Al(NO_3)_3 \cdot 9H_2O$ from Aldrich and $NH_4H_2[NbO(C_2O_4)_3] \cdot xH_2O$ salt supplied by CBMM (Companhia Brasileira de Metalurgia e Mineração). Aluminum nitrate was dissolved in water and oxalic acid was added to reach a pH of 1 and then NH_4OH, to reach a pH of 3. After 15 min stirring, the niobium complex was added in such an amount to reach a Nb/Al

atomic ratio of 1 and a pH of 1.5. The slight blue solution was refluxed for 1 h and water was further removed under vacuum. The white paste was then dried at 423 K for 15 h.

Samples of molybdenum oxide deposited on niobium oxide were prepared by impregnating Nb_2O_5 (prepared by calcining niobic acid sample at 773 K) with an aqueous solution of ammonium heptamolybdate at a pH equal to 5.4 and then calcining it at 773 K in air [18,20]. The theoretical Mo content was equal to 3, 5 and 8 wt.-%.

Vanadyl oxychloride compound ($VOCl_3$ in tetrahydrofuran solution) was grafted on the mixed alumina–niobia samples which were precalcined at 773, 873, 923 and 1023 K, kept in air at room temperature and then heated at 473 K in air before grafting [21,22]. The latter operation was conducted under dry argon atmosphere to avoid moisture. After filtration and washing with dry THF, the solids were hydrolyzed 3 h at 573 K under humid air ($P_{H_2O} = 3 \cdot 10^3$ Pa). The V content, determined by chemical analysis, was equal to 1.2; 0.6; 0.5 and 0.4 wt.-% for precalcination temperature of Al_2O_3:Nb_2O_5 support equal to 773, 873, 923 and 1023 K, respectively.

Infrared studies were carried out using an IFS 110 spectrometer from Bruker and self-supported wafer (about 8 to 30 mg of sample) and controlled atmosphere cells to allow treatment of the samples at given temperatures and atmospheres.

XPS measurements were performed with an Hewlett Packard HP 5950 A spectrometer. The powder samples were deposited on an indium foil, pressed and then transferred into the vacuum chamber without further treatment.

Microanalysis of the elemental composition of the solids was performed using an EDX–STEM high resolution electron microscope HB5 from Vacuum Generator.

^{27}Al MAS–NMR spectra were recorded on a Bruker MSL-300 spectrometer by using a single pulse sequence. Chemical shifts were referred to $Al(H_2O)_6^{3+}$ peak.

Calorimetric measurements were performed using a Tian Calvet type microcalorimeter from Setaram attached to an adsorption equipment [20]. Before NH_3 adsorption, the samples were outgassed at the desired calcination temperature. NH_3 as a basic probe molecule was added stepwise by introducing in the cell small doses of known amount at 373 K.

Catalytic test reactions were performed in a flow microreactor using 100 to 350 mg of catalyst. The unconverted reactants and the products were analyzed by on-line gas phase chromatography.

Isopropanol conversion (3% in air or in N_2, total flow rate = 30 cm^3 min^{-1}) between 383 and 473 K was studied to characterize acidic, basic and redox properties [6,17]. It can be said that propene formation is attributed to the presence of acid sites (Brønsted or Lewis), acetone formation in absence of O_2 (dehydrogenation) to the presence of basic sites and acetone formation in presence of O_2 (oxidehydrogenation) to the presence of redox sites. In order to compare the activities of all samples studied in this work, the intrinsic rates of propene and acetone formation were measured at 443 K. When it was necessary, extrapolation was made using activation energy values equal to 104 and 70 kJ mol^{-1} for propene and acetone, respectively [20].

The oxidative behavior of MoO_x and VO_x supported catalysts were determined by their catalytic activity in, respectively, partial oxidation of propene at 628 K ($C_3^=$:O_2:N_2 = 13:13:74, total flow rate = 60 cm^3 min^{-1}) and oxidative dehydrogenation of propane at 773 K (C_3:O_2:N_2 = 2:19.6:78.4, total flow rate = 50 cm^3 min^{-1}).

3. Results and discussion

3.1. Niobic acid and niobic oxide

Niobic acid was calcined at increasing temperatures from 383 to 773 K under N_2 flow

giving samples Nb_1 to Nb_5 as referenced in Table 1. The samples were shown by XRD to be amorphous up to 773 K where only some peaks of γ-Nb_2O_5 appeared. For Nb_1 sample, two endothermic peaks in DTA at 398 and 473 K were attributed to the elimination of adsorbed and crystallization water molecules, respectively, and an exothermic peak at 848 K attributed to the crystallization of γ-Nb_2O_5.

Acidic properties, determined by microcalorimetry of NH_3 adsorption at 373 K [20], are summarized in Table 1. It appears that the superficial acidity was roughly constant in amount and strength, up to 673 K and decreased sharply above, in amount as well as in strength. Note that the number of acid sites is rather low (ca. 1.6–1.7 molecules nm^{-2}) with respect to the expected value of 8–12 for a complete hydroxyl coverage as observed for many oxides as SiO_2, Al_2O_3 [23], etc.

Isopropanol conversion reaction was studied in presence of N_2 or air as carrier gas, in conditions of non-diffusional regime and at low conversion extent.

It has to be noted that $Nb_2O_5 \cdot xH_2O$ exhibits only the features of an acid solid, since its selectivity is 100% towards propene formation. The intrinsic rate of propene formation increased (Fig. 1 and Table 2) when the calcination temperature increased from 473 to 573 K, then it was stable up to 673 K and strongly decreased above. The amount of acid sites as determined by microcalorimetry only varied slightly between 473 and 673 K, while the turn-over frequency (TOF) values, as calculated, assuming that the active sites are those measured by microcalorimetry, went through a maximum. Then, it can be suggested that the strength

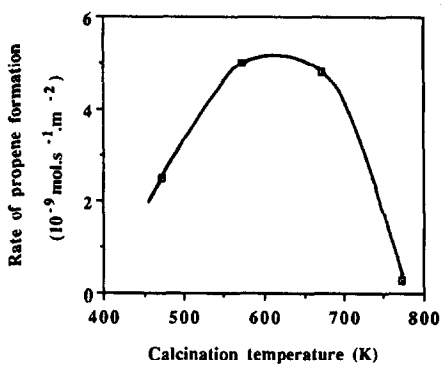

Fig. 1. Variations of the intrinsic rate of propene formation versus the calcination temperature of niobic acid for isopropanol conversion in N_2 at 443 K.

Table 1
Influence of the calcination temperature of $H_8Nb_6O_{19} \cdot xH_2O$ sample on its surface area and its acidic properties as determined by microcalorimetry of NH_3 adsorption at 373 K

Samples	Calcination temperature (K)	Surface area ($m^2\ g^{-1}$)	NH_3 adsorption [20]	
			Concentration (μmol m^{-2})	Initial diff. heat (kJ mol^{-1})
Nb_1	383	140	–	–
Nb_2	473	104	2.8	160
Nb_3	573	86	2.7	196
Nb_4	673	64	2.8	168
Nb_5	773	35	1.2	86

Table 2
Catalytic activity of $Nb_2O_5 \cdot xH_2O$ samples in isopropanol conversion at 443 K, in the presence of N_2 or air as carrier gas

Samples	Calcination temperature (K)	Rate of propene formation (10^{-9} mol s^{-1} m^{-2})	Propene selectivity (%)	TOF [a] (10^{-3} s^{-1})
Nb_2	473	2.5	100	0.9
Nb_3	573	5.0	100	1.9
Nb_4	673	4.8	100	1.7
Nb_5	773	0.3	100	0.3

[a] Value calculated assuming that the active sites are those determined by NH_3 adsorption technique (Table 1).

of the acid sites varied with the calcination temperature. This is quite in agreement with the value of the initial heat of ammonia adsorption (last column in Table 1).

One may propose that for Nb_2 sample the acid sites are $[H(H_2O)_n]^+$ species with a homogeneous distribution of strength. When the temperature calcination increased from 473 to 573 K, the water loss occurred at the expense of these hydrated Brønsted sites with the formation of bare Brønsted sites or of Lewis sites of higher strength. It can be proposed that the activity increase was due not to an increase of the amount of acid sites but rather to an increase of their strength. Above 673 K, reorganization of the Nb_2O_5 lattice, which was achieved with the formation of the γ-Nb_2O_5, strongly decreased the number of acid sites from 2.8 to 1.2 μmol m^{-2} (i.e., 1.7 to 0.7 per nm^2) while their strength was lower as observed both by ammonia adsorption (lower initial heat of adsorption) and by catalytic data (lower TOF values).

In conclusion, one can tell that the water loss during calcination changed the acid properties of $Nb_2O_5 \cdot xH_2O$ from that of a relatively strong acid to that of an oxide with only weak acidity.

3.2. Al_2O_3:Nb_2O_5 mixed oxide

Four samples were prepared by calcining the 1:1 precursor under air flow at 773, 873, 923 and 1023 K and will be designated as $AlNb_1$, $AlNb_2$, $AlNb_3$ and $AlNb_4$, respectively.

Before calcination, the 1:1 molar ratio precursor was studied by IR spectroscopy (1% in KBr pellet) and by DTA–TGA analyses. The IR spectrum of the precursor is dominated by the absorption bands of the oxalate anion and of NH_4^+. By comparison with the alumina and niobia precursors alone, the presence of two bands at 970 cm^{-1} ($\nu_{Nb-O-Al}$ vibration) and 3640 cm^{-1} (ν_{OH} vibration) for the mixed precursor indicates that an interaction between Al and Nb species was existing.

From DTA–TGA analysis of the precursors (using respectively a MDTA 85 Setaram microanalyzer and a 4102 Sartorius microbalance), it appears that the mixed oxide resulted from the decomposition of ammonium and oxalate components in several steps corresponding to the decomposition steps of each single oxides separately. Note, however, that a retarding effect was observed for the decomposition of the Nb oxalate complex with respect to the single oxide precursor (DTA peak shifted from 568 to 593 K). This shows that an interaction between Nb and Al precursors occurred during the formation of the mixed oxide.

The oxalate and ammonium species contained in the precursor were totally decomposed at 623 K [19] and only water loss was observed above 673 K.

The X-ray diffraction patterns shown in Fig. 2 for the calcined samples indicate that the materials are amorphous at calcination temperature up to 923 K. At 1023 K well crystallized aluminum niobate was obtained.

The physicochemical properties for the four calcined samples are given in Table 3. The decrease of the surface area is accompanied by a shift of the mean pore diameter from 7 nm for

Table 3
Physicochemical properties of Al_2O_3:Nb_2O_5 (1:1) mixed oxide sample as a function of calcination temperature

Samples	Calcination temperature (K)	Surface area (m^2 g^{-1})	OH content [a] (μmol nm^{-2})	Al/Nb atomic ratio	
				Chem. analysis	XPS
$AlNb_1$	773	168	2.1	1.1	1.3
$AlNb_2$	873	115	2.0	1.1	–
$AlNb_3$	923	95	1.5	1.1	–
$AlNb_4$	1023	53	0.9	1.0	1.2

[a] Calculated from TGA data (water loss between 473 and 1073 K).

solids $AlNb_1$ and $AlNb_2$ to 9 and 11 nm for $AlNb_3$ and $AlNb_4$, respectively.

Increase of the calcination temperature resulted in a decrease of the superficial OH concentration as determined by TGA analyses. It is noted that the hydroxyl coverage is rather small as compared to silica or alumina with high surface area which contain 13 to $20 \cdot 10^{-6}$ OH per m^2 [23].

The presence of hydroxyl groups was confirmed by IR spectroscopy. The solids in the form of thin self-supported wafers were treated in the IR cell under O_2 at the calcination temperature described above and then outgassed at 423 K. In the 3900–3300 cm^{-1} range, several hydroxyl bands were observed at 3820, 3730, 3690, 3580, 3485, 3410 and 3345 cm^{-1} for samples $AlNb_1$ to $AlNb_3$ [19]. For sample $AlNb_4$, only weak bands were observed at 3825, 3680, 3500 and 3345 cm^{-1}. The bands observed for the samples $AlNb_1$ to $AlNb_3$ correspond to both those of alumina and niobate as if each component was keeping its own oxide individuality. The weak intensity of the OH bands for $AlNb_4$ is correlated to the formation of the well crystallized $AlNbO_4$ phase.

XPS analyses show a slight superficial enrichment in Al of mixed oxide crystallites, with binding energy values of 530.4 eV with a shoulder at 532.1 eV for O 1s peak of sample $AlNb_1$ and a single peak at 530.5 eV for sample $AlNb_4$ while for niobia and alumina the O 1s peak was observed, respectively, at 529.8 and 531.8 eV. This indicates that for the mixed oxide, one has an average value between niobia and alumina, value equal to that of aluminum niobate, the peak at 532.2 eV being indicative to the presence of OH species.

Nb 3 $d_{5/2}$ and 3 $d_{3/2}$ lines were observed, respectively at 207 and 209.7 eV for sample $AlNb_1$ and 207.2 and 209.9 eV for sample $AlNb_4$ against 207.6 eV for Nb $3d_{5/2}$ of Nb_2O_5.

Al 2p lines were found at 73.9 and 74.0 eV for $AlNb_1$ and $AlNb_4$, respectively, against 74.5 eV for alumina.

All these XPS data unless a slight surface enrichment in Al suggest the presence of an aluminum niobate phase, more or less hydrated on the surface of all samples, even when it is amorphous, i.e., below 1023 K. The hydroxyl groups appear to be those of both oxides individually (vide supra).

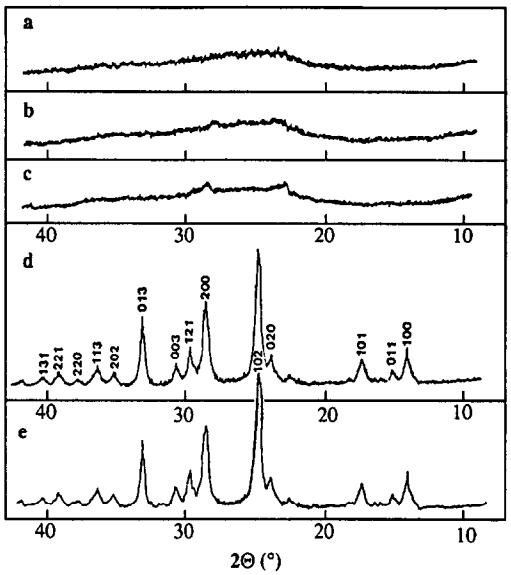

Fig. 2. X-Ray diffraction patterns of Al_2O_3:Nb_2O_5 mixed oxide for different calcination temperatures. (a) 773 K: $AlNb_1$, (b) 873 K: $AlNb_2$, (c) 923 K: $AlNb_3$, (d) 1023 K: $AlNb_4$ and (e) $AlNbO_4$.

An EDX–STEM analysis, using a VG HB5 electron microscope, indicates a narrow distribution of Al/Nb atomic ratio values around 0.95 ± 0.2 against 1.09 from chemical analysis with only a few domains rich in aluminum. These data are consistent with the presence of an homogeneous mixed oxide in a ratio Al_2O_3:Nb_2O_5 close to 1, with only a few particles of alumina alone which are either in small particles or deposited at the surface of the mixed oxide particles as determined by XPS.

The ^{27}Al MAS–NMR spectra of the samples $AlNb_1$, $AlNb_2$ and $AlNb_3$ (Fig. 3) were similar to that of alumina with peaks at ca. 60, 30 and 0 ppm usually attributed respectively, to tetra, penta (or distorted tetra) and hexacoordinated aluminum cation [19]. This indicates that alumina component of the mixed oxide seems to keep its own individuality. At variance, the spectrum of $AlNb_4$ showed only one peak at

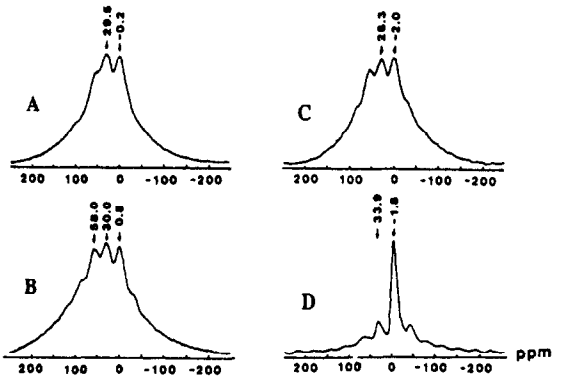

Fig. 3. ^{27}Al MAS–NMR spectra of samples (a) $AlNb_1$, (b) $AlNb_2$, (c) $AlNb_3$ and (d) $AlNb_4$.

−1.8 ppm attributed to octahedral aluminum in the crystalline $AlNbO_4$ phase.

For isopropanol conversion reaction with N_2 as carrier gas, propene was the only product detected. Therefore, it can be concluded that the samples exhibit only acidic properties. In Table 4, the data obtained at 443 K are reported. It is observed that all samples present similar intrinsic activity (third column) and that $AlNb_4$, which is in the form of a well crystallized $AlNbO_4$ compound, is only slightly less active. Comparing with the Nb_2O_5 sample calcined at 773 K (Table 2), one can conclude that, in good agreement with the prediction, the mixed oxide samples are more acidic than the single oxide since the intrinsic rate of propene formation increases from $0.3 \cdot 10^9$ mol s^{-1} m^{-2} for Nb_5 to 1.3 ± 0.3 for samples $AlNb_1$ to $AlNb_4$. It is noted that for the 773 K calcined samples Nb_5 and $AlNb_1$, the turn-over frequency values are identical ($0.3 \cdot 10^{-3}$ s^{-1}) indicating that the two samples differ only by the number of acid sites. At variance, TOF values increased from 0.3 to 0.8 with increasing calcination temperature as if the nature of the acid sites were modified.

3.3. MoO_x on Nb_2O_5 catalysts

The main characteristics of the samples obtained by impregnating Nb_2O_5 sample, precalcined at 773 K (referenced as Nb_5), are summarized in Table 5. For comparison, one has also reported the characteristics of a MoO_3 sample with high surface area [24] and its mechanical mixture (5 wt.-% Mo) with Nb_5.

Table 4
Catalytic activity of Al_2O_3:Nb_2O_5 samples in isopropanol conversion at 443 K, with N_2 as carrier gas

Samples	Calcination temperature (K)	Rate of propene formation (10^{-9} mol s^{-1} m^{-2})	Propene selectivity (%)	TOF [a] (10^{-3} s^{-1})
$AlNb_1$	773	1.0	100	0.3
$AlNb_2$	873	1.6	100	0.5
$AlNb_3$	923	1.4	100	0.6
$AlNb_4$	1023	1.2	100	0.8

[a] TOF calculated assuming that the active sites are hydroxyl groups determined by TGA data.

Table 5
Physicochemical properties of Mo/Nb_5 samples

Samples	Mo content		Surface area (m^2 g^{-1})	Adsorption of NH_3 at 373 K	
	(wt.-%)	(μmol m^{-2})		Concentration (μmol m^{-2})	Initial diff. heat (kJ mol^{-1})
Nb_5	0	0	35	1.2	86
Mo_1/Nb_5	3	9.8	32	2.3	130
Mo_2/Nb_5	5	13.8	38	2.7	145
Mo_3/Nb_5	8	21.3	39	2.2	135
MoO_3	66.7	11.8 [a]	44	0.8	40
Mixture [b]	5	21.3	26	–	–

[a] Theoretical monolayer coverage corresponds to 11.8 μmol m^{-2}, assuming that each molybdenum species occupies about 0.14 nm^2 [20].
[b] Mechanical mixture of MoO_3 and Nb_5 with 5 wt.-% Mo.

In the X-ray diffraction patterns of impregnated samples, only the lines of the γ-Nb_2O_5 phase were detected, even for the highest Mo content. In contrast, the X-ray diffraction pattern of a mechanical mixture of MoO_3 and Nb_2O_5 (5 wt.-% Mo) contained detectable peaks of MoO_3 besides those of Nb_2O_5. This indicates that for all impregnated samples MoO_x species is rather well dispersed on Nb_2O_5.

XPS studies show that the binding energy values for Nb $3d_{3/2}$ and $3d_{5/2}$ (209.8, 207.1) and for Mo $3d_{3/2}$ and $3d_{5/2}$ (235.8 and 232.7 eV) correspond to the values observed for Nb in Nb_2O_5 and Mo in MoO_3. It was observed that the Mo/Nb atomic ratio determined by XPS was four times higher for all impregnated than the chemical ratio, indicating an enrichment in Mo on the surface. However, the Mo spraying appears not to be total, since, much higher ratio values would have been expected by XPS technique for a full dispersion at a coverage close to monolayer (Mo/Nb atomic ratio of several orders of magnitude).

UV–visible and EPR spectroscopies showed that Mo is mainly at the 6^+ oxidation state, in the form of polymeric octahedral species [20] supporting the above XPS data (binding energy values of Mo).

Microcalorimetric data of NH_3 adsorption at 373 K are reported in Table 5 and the variations of the differential adsorption heat versus NH_3 coverage are represented in Fig. 4. It is to be noted that the Mo spraying on the Nb_2O_5 surface generates strong acid sites which amounts are not proportional to the Mo loading, confirming that the dispersion is only partial. The values of the initial differential adsorption heat are three times higher on impregnated samples than on MoO_3, indicating that the superficial molybdate species have specific properties (higher acidic strength) different from that of bulk MoO_3.

A SIMS study, reported in Ref. [25], showed that Mo^+/Nb^+ ratio increased linearly with Mo loading up to 3 wt.-% and then less than expected from a linear increase. As this technique

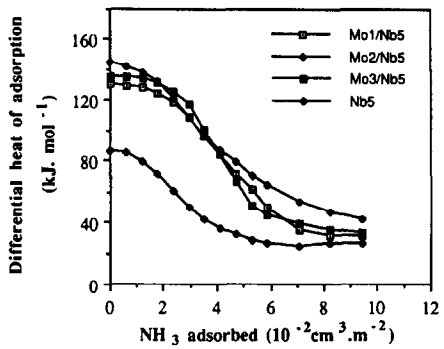

Fig. 4. Variations of the differential heat of NH_3 adsorption at 373 K versus coverage on Mo/Nb_5 samples. (a): Nb_5, (b): Mo_1/Nb_5, (c): Mo_2/Nb_5 and (d): Mo_3/Nb_5.

is sensitive to the first atomic layer of a crystallite while XPS is sensitive to several layers (2 to 5 nm depth), it can thus be concluded that MoO_x species are better dispersed at low Mo coverage than at higher coverage in good agreement with the ammonia adsorption data (vide supra) and XPS data. Moreover the MoO^+/Mo^+ ratio decreased with Mo loading instead of being constant. This shows that at low molybdenum loading, the surface MoO_x species are rich in oxygen as if they were containing hydroxyl groups (2 OH instead of 1 Mo = O).

In the infrared spectrum of self-supported Nb_5 sample, outgassed at 373 K, a broad band is observed with two broad maxima at 3450 and 3350 cm^{-1}. Upon molybdate impregnation, a narrow and intense band appeared at 3445 cm^{-1} which disappeared upon outgassing at 523 K. This band resembles that observed for high surface area MoO_3 and attributed to H_2O bonded to Mo^{6+} cation [24]. Upon NH_3 adsorption at room temperature (Fig. 5), the intensity of the 3445 cm^{-1} band decreased without disappearing and new bands were observed at 3360 and 3270 cm^{-1} and at 1605, 1450 and 1215 cm^{-1}. The bands at 3270 and 1450 cm^{-1} correspond to the stretching and bending vibrations of NH_4^+, thus, indicating the presence of Brønsted sites. The bands at 3360 and 1215 cm^{-1} are attributed to the stretching and deformation vibrations of NH_3 coordinated to a Lewis

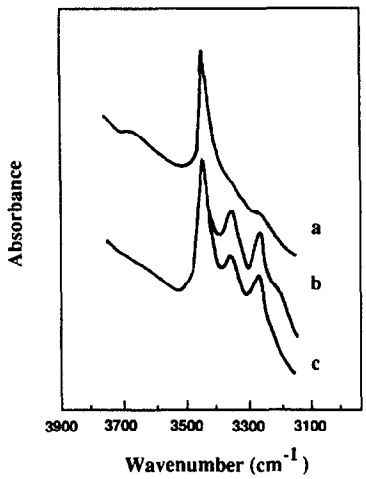

Fig. 5. Infrared spectra of Mo_2/Nb_5, (a) after outgassing at 373 K, (b) after contacted with 1.2 kPa NH_3 at room temperature and outgassing at room temperature, (c) after further outgassing at 373 K.

acid site. All these bands disappeared when the sample was outgassed above 373 K indicating that the Brønsted and Lewis acid sites are not very strong.

3.3.1. Catalytic properties

Isopropanol conversion reaction, in the presence of air, lead to the formation of propene and acetone. Data in Table 6 show that the supported Mo species are much more active for the propene formation than the support alone and exhibit also redox properties. Note also that both propene and acetone intrinsic rates increased with Mo content, while the acidity as determined by NH_3 adsorption remained about the same (column 5 in Table 5).

As for Nb samples, the turn-over frequency values for propene formation were calculated assuming that the acid sites are those determined by NH_3 adsorption. The values obtained (Table 6) are surprisingly very high and increase with the Mo loading. This implies that the mechanism of propene formation is presumably different (acid-base concerted mechanism type E_2 instead of the E_1 mechanism which occurs in presence of Brønsted acidity, see Ref. [17]) and must be related to the MoO_x species. The TOF values calculated per MoO_x species are then equal to 6, 9 and $10 \cdot 10^{-3}$ s^{-1} for Mo_1, Mo_2 and Mo_3/Nb_5 samples, respectively.

For acetone formation, the TOF values, calculated assuming all the Mo atoms are the active sites, increase slightly with the Mo loading.

In propene oxidation reaction (Table 7), the presence of MoO_x species on Nb_2O_5 increased strongly the rate of reaction and improved the selectivity for acrolein. It is to be noted that this selectivity in acrolein was rather low (28%) and was higher for lower Mo content. Then, it decreased for the Mo_3/Nb_5 sample reaching the selectivity of bulk MoO_3. It is interesting to note that the oxidation rate increased with the Mo content in good agreement with the increase

Table 6
Catalytic activity of Mo/Nb_5 samples in isopropanol conversion at 443 K, with air as carrier gas

Samples	Formation rate (10^{-9} mol s^{-1} m^{-2})		Selectivity (%)		TOF [a] (10^{-3} s^{-1})	
	Propene	Acetone	Propene	Acetone	Propene	Acetone
Nb_5	0.3	0	100	0	0.3	
Mo_1/Nb_5	55.9	8.9	86	14	24.3	0.9
Mo_2/Nb_5	129.3	15.2	89	11	47.9	1.1
Mo_3/Nb_5	219.0	31.8	87	13	99.5	1.5
MoO_3	59.2	4.4	93	77	4.0	0.4
Mixture [b]	353.8	14.8	96	4	–	0.7

[a] TOF for propene calculated assuming that the acid sites are those determined by NH_3 adsorption. TOF for acetone calculated assuming that all the Mo atoms are the active sites.

[b] Mechanical mixture of MoO_3 and Nb_5 with 5 wt.-% Mo.

Table 7
Catalytic properties of Mo/Nb_5 samples in propene oxidation at 673 K [20]

Samples	Propene conversion (%)	Conversion rate (10^{-9} mol s^{-1} m^{-2})	Selectivity (%)			TOF [a] (10^{-3} s^{-1}) for acrolein
			Acrolein	CO_2	Other	
Nb_5	0.03	0.5	9	88	3	–
Mo_1/Nb_5	0.13	2.5	26	69	5	0.26
Mo_2/Nb_5	0.21	3.4	28	63	9	0.25
Mo_3/Nb_5	0.53	8.1	14	80	6	0.38
MoO_3	0.29	4.0	15	79	6	0.34
Mixture [b]	0.33	7.7	17	6	7	0.36

[a] TOF calculated assuming that all the Mo atoms are the active sites.
[b] Mechanical mixture of MoO_3 and Nb_5 with 5 wt.-% Mo.

of the acetone formation rate in isopropanol conversion reaction.

In conclusion, it appears that impregnation of Nb_2O_5 by polymolybdate salt results in a good but not an excellent dispersion of the superficial MoO_x species as suggested by XPS and SIMS analyses and in the creation of Brønsted acid sites of moderate acidity. Moreover, it is worthwhile noting that, intrinsic rates for isopropanol conversion and propene oxidation were roughly proportional to total Mo content which implies well dispersed MoO_x species on the surface of Nb_2O_5. As this property was not totally supported by XPS and SIMS analyses, one can suggest that under catalytic reaction conditions, dispersion of MoO_x species was improved as it was observed for mechanical mixture of bismuth molybdate and mixed Co, Fe molybdates under propene oxidation conditions in a kind of wetting process [26,27]. Note also that such molybdenum species strongly enhanced the conversion of isopropanol to propene, that may be due not only to an increase in acidity but mainly to a change in the dehydration mechanism of isopropanol from E_1 to E_2 types [17].

3.4. VO_x on Al_2O_3:Nb_2O_5 catalysts

The samples were prepared by grafting $VOCl_3$ in anhydrous conditions on hydroxyl groups of the mixed oxide samples calcined at different temperatures (samples $AlNb_1$ to $AlNb_4$) as described in the experimental section. The main characteristics of the samples are given in Table 8. The amount of grafted vanadium as determined by chemical analysis is 1.2, 0.61, 0.51 and 0.41 wt.-% for samples $AlNb_1$ to $AlNb_4$, respectively. It is observed that upon grafting, the surface area of the support strongly decreased and that the amount of V by surface area unit equalled 2.7, 2.3, 1.8 and 2.5 μmol m^{-2}, respectively, for the $AlNb_1$ to $AlNb_4$ sam-

Table 8
Catalytic properties of V/AlNb samples in isopropanol conversion at 443 K, with N_2 as carrier gas

Samples	V content (μmol m^{-2})	Rate of formation (10^{-9} mol s^{-1} m^{-2})		Selectivity (%)		TOF [a] (10^{-3} s^{-1})
		Propene	Acetone	Propene	Acetone	Acetone
$AlNb_1$	0	1.0	0	100	0	–
$V/AlNb_1$	2.7	1.5	0.8	89	42	0.8
$V/AlNb_2$	2.3	1.3	1.8	89	42	0.8
$V/AlNb_3$	1.8	2.6	3.4	87	43	1.9
$V/AlNb_4$	2.5	1.4	8.1	15	85	3.2

[a] TOF calculated per vanadium atoms assumed to be the active site and located only at the surface.

ples. These values correspond to a coverage lower than the monolayer, since, one was expecting 5.8 μmol m^{-2} for isolated VO_x species or 16.6 μmol m^{-2} for a bidimensional polyvanadate layer [28]. But, it is noteworthy that the amounts of vanadium are of the same order of magnitude than the amounts of hydroxyl groups (Table 3).

In fact, infrared studies of self-supported wafers showed in the 3900–3300 cm^{-1} range the disappearance of the bands at 3730, 3690 and 3485 cm^{-1} and a decrease of the bands near 3525 and 3410 cm^{-1} for sample $AlNb_1$ and a strong decrease of all hydroxyl bands for sample $AlNb_4$. This shows clearly that the grafting occurred at the expense of hydroxyl groups.

3.4.1. Catalytic properties

For isopropanol conversion reaction with N_2 as carrier gas, it is interesting to note that the rates of propene formation was approximate the same than for the bare support (column 3, Table 4 and column 3, Table 8) while acetone was formed in increasing amounts when the precalcination temperature of the support increased from 773 to 1023 K. It then follows that the propene and acetone selectivities changed from one sample to the other. Note that such a behavior is different from that of Mo_x/Nb_2O_5 for which the mechanism of propene formation from isopropanol was suggested to be different compared to Nb_2O_5 samples.

Propane oxidation was performed at 773 K. The experimental data are given in Table 9. It is clear that propane conversion intrinsic rate was similar for all AlNb samples with low selectivity in propene, particularly for $AlNb_4$ sample which contains primarily $AlNbO_4$ phase. Upon grafting VO_x species in the range of 1.8 to 2.7 μmol m^{-2}, the conversion rate sharply increased and the selectivity in propene also, particularly for $AlNb_2$ and $AlNb_3$ supports.

Considering the experimental results for both isopropanol conversion and propane oxidation reactions, it can be suggested that isopropanol conversion into propene only occurs on the bare AlNb support since VO_x coverage is rather low (in the order of 15%) while the VO_x species exhibit redox properties as observed for isopropanol conversion to acetone and for propane oxidative dehydrogenation to propene, the bare support exhibiting relatively low activity. Note then that the VO_x species on well crystallized $AlNbO_4$ support ($AlNb_4$ sample) exhibits the highest intrinsic rate of acetone formation in isopropanol conversion and the highest intrinsic rate of propene formation in propane oxidation reaction in spite of a lower selectivity.

Since, the VO_x coverage is almost the same for all the samples, the increase of the TOF values for acetone formation from isopropanol and for propene formation from propane may be explained by a difference in the nature of these VO_x species and more particularly by their condensation degree, induced by the crystallization of the $AlNbO_4$ phase. It could be related to an

Table 9
Catalytic properties of V/AlNb samples in propane oxidation at 773 K

Samples	Conversion (%)	Conversion rate (10^{-9} mol s^{-1} m^{-2})	Selectivity (%)			TOF [a] (10^{-3} s^{-1}) into propene
			Propene	CO	CO_2	
$AlNb_1$	3.7	0.8	10	0	88	–
$V/AlNb_1$	11.8	5.2	12	0	87	1.9
$AlNb_2$	3.1	0.9	8	7	85	–
$V/AlNb_2$	9.2	4.4	65	33	2	1.9
$AlNb_3$	2.8	0.6	6	10	83	–
$V/AlNb_3$	10.4	3.6	62	21	16	2.0
$AlNb_4$	1.8	0.9	3	18	64	–
$V/AlNb_4$	11.5	16.3	44	25	18	6.5

[a] TOF calculated assuming that the active sites are V atoms on the surface.

epitaxial grafting of VO_x species on the mixed Al_2O_3:Nb_2O_5 support which crystallized more and more into well organized $AlNbO_4$ material when the precalcination temperature of the support increased from 773 to 1023 K (samples $AlNb_1$ to $AlNb_4$). Such a structure sensitivity for oxidation reactions has already been largely demonstrated, even if the condensation degree of the VO_x species is hardly determined by physical means. It corresponds, nevertheless, to a general trend for partial oxidation reactions.

Note, however, that in Ref. [29] in this issue of Catalysis Today, different results were described for VO_x species supported on Nb_2O_5 which do not exhibit structure sensitivity for propane oxidative dehydrogenation at 773 K.

4. Conclusions

Niobic acid has been clearly shown to exhibit strong acidic properties and to dehydroxylate upon calcination above 673 K resulting in a weakly acidic Nb_2O_5 oxide.

Coprecipitation of Al_2O_3:Nb_2O_5 in a 1:1 molar ratio results in a mixed oxide which exhibits higher acidic properties than niobia or alumina alone, following Tanabe's predictions, but of relatively moderate strength. Upon calcination, the mixed oxide transforms into a well crystallized aluminum niobate compound of more moderate acidity.

Deposition of MoO_x species on niobia generates catalytic oxidation properties and also creates some new Brønsted type acid sites. Unfortunately, the selectivity in partial oxidation of propene is low, which is certainly due to the presence of Brønsted acid sites. Moreover, it is proposed that MoO_x species dispersion was indeed not excellent but was improved during the catalytic reaction by a kind of wetting effect of the active species on the oxidic support.

For isopropanol dehydration to propene, it is suggested that the surface molybdenum species lead to an E_2-type mechanism different from the E_1-type on the bare support and are particularly efficient for the reaction.

Upon grafting VO_x species on the mixed oxide Al_2O_3:Nb_2O_5, precalcined at increasing temperatures to get a more and more crystallized support, one gets catalysts which exhibit moderate acidic properties as the bare supports but more importantly redox and, subsequently, interesting partial oxidation reaction properties. As the TOF values increased with the crystallization state of the support, it is suggested that the condensation of VO_x species varied with the crystallization degree of the support favoring a kind of epitaxial growth of VO_x species which results in better partial oxidation properties.

References

[1] K. Tanabe (Editor), Catal. Today, 16(3–4) (1993).
[2] Y. Higashio and T. Nakayama, Eur. Pat. 227868, 1985.
[3] T. Iizuka, K. Ogasawara and K. Tanabe, Bull. Chem. Soc. Jpn., 56 (1983) 2927.
[4] Z. Chen, T. Iizuka and K. Tanabe, Chem. Lett., (1984) 1085.
[5] K. Tanabe, T. Sumiyoshi, K. Shibata, T. Kiyoura and J. Kitagawa, Bull. Chem. Soc. Jpn., 47 (1974) 1064.
[6] K. Tanabe, M. Misono, Y. Ono and H. Hattori (Editors), Stud. Surf. Sci. Catal., 51 (1989) 108.
[7] M. Itoh, H. Hattori and K. Tanabe, J. Catal., 35 (1974) 225.
[8] Z. Liu, J. Tabora and R.J. Davis, J. Catal., 149 (1994) 117.
[9] J.R. Sohn, H.J. Jang, M.Y. Park, E.H. Park and S.E. Park, J. Mol. Catal., 93 (1994) 149.
[10] H.J.M. Bosman, E.C. Kruissink, J. van der Spoel and F. van den Brink, J. Catal., 148 (1994) 660.
[11] J.B. Miller, S.E. Rankin and E.I. Ko, J. Catal., 148 (1994) 682.
[12] S.M. Maurer, D. Ng and E.I. Ko, Catal. Today, 16 (1993) 319.
[13] T. Seiyama, Metal Oxides and Their Catalytic Actions, Kodansha, Tokyo, 1978.
[14] B.F. Pedersen, Acta Chem. Scand., 16 (1962) 421.
[15] R. Marchand, L. Brohan and M. Tournoux, Mat. Res. Bull., 15 (1980) 1129.
[16] R. Rohmer, in P. Pascal (Editor), Nouveau Traité de Chimie Minérale, Masson, Paris, 1958.
[17] A. Ouqour, G. Coudurier and J.C. Védrine, J. Chem. Soc., Faraday Trans., 89 (1993) 3151.
[18] A. Ouqour, PhD Thesis, University of Lyon, 1991, No. 105-91.
[19] P.G. Pries de Oliveira, F. Lefebvre, M. Primet, J.G. Eon and J.C. Volta, J. Catal., 130 (1991) 293.
[20] Y.S. Jin, A. Ouqour, A. Auroux and J.C. Védrine, Stud. Surf. Sci. Catal., 48 (1989) 525.
[21] P.G. Pries de Oliveira, F. Lefebvre, J.G. Eon and J.C. Volta, J. Chem. Soc., Chem. Comm., (1990) 1480.

[22] P.G. Pries de Oliveira, J.G. Eon and J.C. Volta, J. Catal., 137 (1992) 257.
[23] J.B. Peri, J. Phys. Chim., 69 (1965) 211 and 220.
[24] P. Vergnon, D. Bianchi, R. Benali Chaoui and G. Coudurier, J. Chim. Phys., 77 (1980) 1043.
[25] Y.S. Jin, A. Auroux and J.C. Védrine, J. Chem. Soc., Faraday Trans. 1, 85 (1989) 4179.
[26] H. Ponceblanc, J.M.M. Millet, G. Coudurier and J.C. Védrine, ACS Symp. Ser., 523 (1993) 262.
[27] J.M.M. Millet, H. Ponceblanc, G. Coudurier, J.M. Herrmann and J.C. Védrine, J. Catal., 142 (1993) 381.
[28] G.C. Bond and J.C. Védrine, Catal. Today, 20 (1994) 171.
[29] T.C. Watling, G. Deo, K. Seshan, I.E. Wachs and J.A. Lercher, Catal. Today, 28 (1996) this issue.